Performance Analysis of Visible Light Communications with Channel Blockage Caused by Human Bodies

Xiping Wu

School of Electrical and Electronic Engineering
University College Dublin, Dublin, D04 V1W8, Ireland
xiping.wu@ucd.ie

***Abstract*—This work studies the impact of channel blockage caused by human bodies in visible light communications (VLC), which is one of the key wireless technologies in 6G. As operating on the optical spectra, VLC channels can be blocked by opaque objects, especially by human users themselves. This human blockage has a nonnegligible impact on the performance of VLC. The current literature mostly considers human bodies as shaped objects to evaluate the numerical performance of VLC. In this paper, the coverage probability of line-of-sight (LoS) signal-to-noise ratio (SNR) under the impact of human blockage is derived in a closed-form expression and validated against simulations. The impact of human blockage on non line-of-sight (NLoS) is also analysed in specific room environments. Results show that increasing the distance between body and device from 10cm to 30cm can nearly halve the blockage probability, from 22% to 12%. Also, a shorter separation between VLC APs can effectively mitigate the LoS SNR degradation caused by human blockage, while the NLoS SNR degradation is irrelevant to the APs' separation.**

***Index Terms*—Visible light communication (VLC), light fidelity (LiFi), channel blockage, SNR coverage probability**

I. Introduction

With imminent standards such as IEEE 802.11bb and ITU G.9991, visible light communications (VLC) are on the way to commercial use in the six generation (6G). Based on the existing light infrastructure, VLC can fulfil simultaneous illumination and communication to help reduce the carbon footprint of the information and communication technology (ICT) sector. In addition, VLC provides a number of other advantages over radio frequency (RF) systems, including: i) offering wide and unregulated visible spectrum, ii) feasibility in RF-restricted areas, and iii) rendering secure communication in opaque compartments [1]. Recent studies show that with a single phosphorescent white light-emitting diode (LED), it is able to achieve a VLC link data rate above 1 Gbit/s [2]. Moreover, VLC can be combined with the existing RF systems, forming a hybrid network to greatly improve the capacity of wireless communications [3].

Meanwhile, VLC is susceptible to channel blockage caused by opaque objects, particularly the bodies of human users. This is referred to as human blockage, which has been widely considered in access point selection (APS) and load balancing for VLC [4] and VLC-related hybrid networks [5], [6]. The handover process was studied for VLC in [4], which shows that blockage would increase the handover rate more noticeably for slow-moving users than fast-moving users. As for hybrid VLC and RF networks, when blockage occurs to a VLC user, it can be transferred to an RF access point (AP) or another VLC AP of which the link is not blocked. A support vector machine-based scheme was proposed in [5] to determine the type of network access, by exploiting the temporal correlation of blockage parameters. In [6], load balancing for the hybrid VLC and RF network is formulated as an optimisation problem, which characterises blockage in the objective function.

In the above studies, channel blockage is modelled as a Poisson process with key parameters to describe how often blockage occurs and how long blockage lasts. However, this type of model does not reflect how human bodies impose blockage to the device. Some studies have been carried out to model human blockage. The authors in [7] established an empirical probabilistic model of blockage events. However, this model does not directly reflect how human body causes blockage. In [8], the human body is modelled as a slab obstacle with a certain height and width. This model only fits a simple scenario where the obstacle is exactly inbetween the AP and the device. In [9], human bodies are modelled as a cylinder object, and the length of shadow is used for computing the chance of blockage. Similar to [8], [9] is under an unrealistic assumption that the device, the human body, and the AP are in a line. The cylinder model was also adopted in [10], which derived the blockage probability for a given distance between human body and AP, by computing the threshold of the angle between the human body and the device. However, this work has two major limitations: i) it fails to address the impact of the distance between human body and device, and ii) it considers line-of-light (LoS) only and does not reflect the impact of human blockage on non line-of-sight (NLoS).

In VLC, LoS typically contributes a large portion of the received signal power [11]. In this paper, a closed-form expression is derived for the coverage probability of LoS signal-to-noise ratio (SNR) under the impact of human blockage, particularly involving the distance between human body and device. Results show that increasing the distance between body and device from 10cm to 30cm can nearly halve the blockage probability, from 22% to 12%. Apart from that, reducing the

APs' separation can effectively mitigate the LoS SNR degradation caused by human blockage. Unlike LoS, the impact of human blockage on NLoS depends on the room environment. While it is difficult to derive the coverage probability of NLoS SNR under the impact of human blockage, numerical results are analysed. It is found that the NLoS SNR degradation is irrelevant to the APs' separation.

The remainder of this paper is organised as follows. The VLC system model and channel model are introduced in Section II. In Section III, the coverage probability of LoS SNR is derived in closed-form, based on blockage modelling and the derivation of blockage probability. Simulation results are presented in Section IV to validate the theoretical derivation. The impact of human blockage on LNoS SNR is also analysed in this section. Finally, conclusions are drawn in Section V.

II. System Model

The VLC APs are integrated into ceiling LED lamps, which are deployed in a lattice. Given a user, there are 4 nearest VLC APs, and the user is usually connected to one of them. Hence, only a set of 4 VLC APs need to be considered to model human blockage. The APs employ different spectra and thus do not interfere with each other. As for the user equipment (UE), it has a single photodiode (PD) facing upwards. Without loss of generality, downlink is considered in this paper. The analysis also applies to uplink due to the law of reversibility of light. The VLC channel is comprised of LoS and NLoS paths. The channel gain of LoS can be written as follows [12, eq. (10)]:

$$H_{i,u}^{\text{LoS}} = \frac{(m+1)A_{\text{pd}}}{2\pi d_{i,u}^2}\cos^m(\phi_{i,u})g_f g_c \cos(\psi_{i,u}), \tag{1}$$

where $m = -\ln 2/\ln(\cos\Phi_{1/2})$ represents the Lambertian emission order, and $\Phi_{1/2}$ is the angle of half intensity; A_{pd} is the physical area of the PD; $d_{i,u}$ denotes the Euclidean distance between AP i and user u; $\phi_{i,u}$ and $\psi_{i,u}$ are the angles of radiance and incidence; g_f denotes the optical filter gain; and the concentrator gain g_c is given by [12, eq. (8)]:

$$g_c = \begin{cases} \dfrac{n^2}{\sin^2(\Psi_{\text{max}})}, & 0 \le \psi_{i,u} \le \Psi_{\text{max}} \\ 0, & \psi_{i,u} > \Psi_{\text{max}} \end{cases}, \tag{2}$$

where n is the refractive index, and Ψ_{max} denotes the semi-angle of the field of view (FoV) of the PD.

As for the NLoS component, only first-order reflections are taken into account as higher-order reflections typically contribute little [12]. A first-order reflection is comprised of two segments: a) from the AP to a small area w on the wall, and b) from w to the user. Let $d_{i,w}$ and $d_{w,u}$ denote the Euclidean distances of the two segments. The angles of radiance and incidence in the first segment are $\phi_{i,w}$ and $\vartheta_{i,w}$, while they are $\vartheta_{w,u}$ and $\psi_{w,u}$ in the second segment. Let A_w denote the area of w, and the wall reflectivity is ρ_w. The channel gain of NLoS is given by (3) [12, eq. (12)]. The total channel gain is $H_{i,u} = H_{i,u}^{\text{LoS}} + H_{i,u}^{\text{NLoS}}$.

At the receiver, the PD converts the captured photons into an electric current:

$$I_{\text{elec}} = R_{\text{pd}} H_{i,u} P_{\text{mod}}, \tag{4}$$

where R_{pd} is the detector responsivity while P_{mod} is the transmit optical power used for modulation. Let $\dot{\gamma}_{i,u}$ denote the received SNR of the UE without channel blockage:

$$\dot{\gamma}_{i,u} = \frac{(R_{\text{pd}} H_{i,u} P_{\text{mod}})^2}{N_{\text{VLC}} B_{\text{VLC}}}, \tag{5}$$

where N_{VLC} is the power spectral density (PSD) of noise at the receiver, including shot noise and thermal noise, and B_{VLC} is the bandwidth per VLC AP.

III. Coverage Probability Analysis of LoS SNR

In this section, the impact of human blockage on SNR coverage probability is theoretically derived for LoS. The impact on NLoS is difficult to derive since it depends on specific room environments. Alternatively, numerical results are presented in Section IV with a detailed setup for NLoS.

A. Blockage Modelling

Fig. 1 illustrates LoS blockage caused by the human user. The human body is usually modelled by a cylinder object, of which the diameter is d_H. Let h_H denote the height of the cylinder, which is the vertical distance between the top of the cylinder and the UE. The human user holds the UE in front of the body in a certain distance. Thus, it is modelled that the UE is positioned at a random point in a circle around the human body, with radius r_H. Let $h_{i,H}$ and $l_{i,H}$ denote the vertical and the horizontal distances between the AP and the human user, respectively. As shown in Fig. 1, the shadow of the human body can be approximated to be a trapezoid, of which the top base is d_H. Let l_b, l_c and l_s denote the bottom base, the height, and the side of the trapezoid, respectively. The parameters l_b and l_c can be readily obtained by:

$$l_b = \frac{h_{i,H} d_H}{h_{i,H} - h_H}. \tag{6}$$

$$l_c = \frac{h_H l_{i,H}}{h_{i,H} - h_H}. \tag{7}$$

The parameter l_s is determined by:

$$l_s = \sqrt{\left(\frac{l_b - d_H}{2}\right)^2 + l_c^2}. \tag{8}$$

Substituting (6) and (7) into the above equation, it gives:

$$l_s = \frac{h_H}{h_{i,H} - h_H}\sqrt{\left(\frac{d_H}{2}\right)^2 + l_{i,H}^2}. \tag{9}$$

B. Blockage Probability

The LoS path is blocked when the UE is located in the shadow area shown in Fig. 1. To derive the blockage probability of LoS, three cases are considered: i) $r_H \ge l_s$; ii) $r_H \le l_c$; and iii) $l_c < r_H < l_s$.

$$H_{i,u}^{\mathrm{NLoS}} = \int_{A_w} \frac{(m+1)A_{\mathrm{pd}}}{2(\pi d_{i,w} d_{w,u})^2} \rho_w \cos^m(\phi_{i,w}) g_f g_c \cos(\psi_{w,u}) \cos(\vartheta_{i,w}) \cos(\vartheta_{w,u}) dA_w. \tag{3}$$

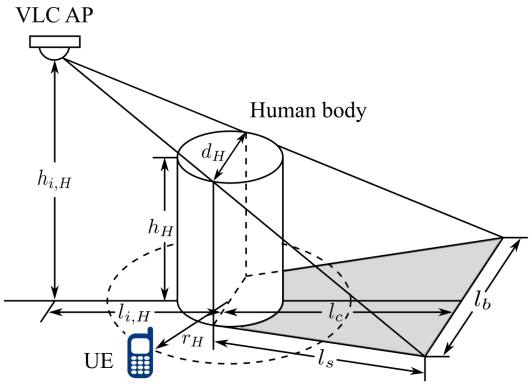

Fig. 1. Schematic diagram of LoS blockage.

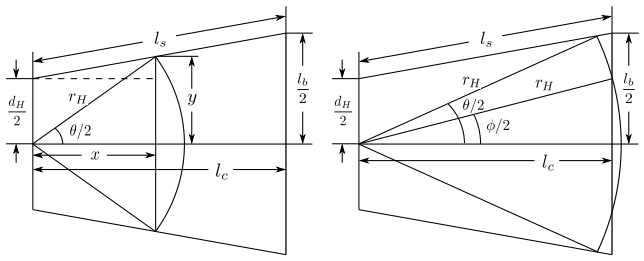

(a) $r_H \leq l_c$ (b) $l_c < r_H < l_s$

Fig. 2. Blockage situations of LoS.

1) $r_H \geq l_s$*:* In this case the UE is always outside the shadow area. Substituting (9) into $r_H \geq l_s$, we have:

$$l_{i,H} \leq \sqrt{\left[\frac{r_H(h_{i,H}-h_H)}{h_H}\right]^2 - \left(\frac{d_H}{2}\right)^2} = l_1. \tag{10}$$

2) $r_H \leq l_c$*:* In this case the UE might fall in the shadow area, and the blockage probability depends on the arc angle of the UE orbit inside the shadow area. Let θ denote the arc angle. As shown in Fig. 2(a), there exists:

$$\frac{x}{y - \frac{d_H}{2}} = \frac{l_c}{\frac{l_b}{2} - \frac{d_H}{2}}, \tag{11}$$

where $x = r_H \cos(\theta/2)$ and $y = r_H \sin(\theta/2)$. This gives:

$$\sin\left(\frac{\theta}{2}\right) = \frac{2\alpha d_H + \sqrt{(4\alpha+1)r_H^2 - \alpha d_H^2}}{(4\alpha+1)r_H}, \tag{12}$$

where:

$$\alpha = \left(\frac{l_c}{l_b - d_H}\right)^2. \tag{13}$$

Substituting (6) and (7) into the above equation, it gives:

$$\alpha = \left(\frac{l_{i,H}}{d_H}\right)^2. \tag{14}$$

Therefore, θ can be obtained as follows:

$$\theta = 2\arcsin\left(\frac{2\alpha + \sqrt{\eta_H^2(4\alpha+1) - \alpha}}{\eta_H(4\alpha+1)}\right), \tag{15}$$

where $\eta_H = \frac{r_H}{d_H}$. To satisfy $r_H \leq l_c$, there exists:

$$l_{i,H} \geq \frac{r_H(h_{i,H}-h_H)}{h_H} = l_2. \tag{16}$$

The blockage probability in this case can be written as:

$$\mathbb{P}_{\mathrm{B}}(l_{i,H} | l_{i,H} \geq l_2) = \frac{\theta}{2\pi}. \tag{17}$$

3) $l_c < r_H < l_s$*:* In this case the arc angle that makes the UE fall in the shadow area is $\theta - \phi$, as shown in Fig. 2(b). The angle θ has been derived in (15), whereas ϕ can be computed by:

$$\phi = 2\arccos\left(\frac{l_c}{r_H}\right). \tag{18}$$

Substituting (7) into the above equation, it gives:

$$\phi = 2\arccos\left(\frac{h_H l_{i,H}}{(h_{i,H}-h_H)r_H}\right). \tag{19}$$

The corresponding blockage probability is given by:

$$\mathbb{P}_{\mathrm{B}}(l_{i,H} | l_1 < l_{i,H} < l_2) = \frac{\theta - \phi}{2\pi}. \tag{20}$$

Combining the above three cases, the blockage probability of LoS can be derived as a function of $l_{i,H}$:

$$\mathbb{P}_{\mathrm{B}}(l_{i,H}) = \begin{cases} 0, & \text{when } l_{i,H} \leq l_1 \\ \dfrac{\theta - \phi}{2\pi}, & \text{when } l_1 < l_{i,H} < l_2 \\ \dfrac{\theta}{2\pi}, & \text{when } l_{i,H} \geq l_2 \end{cases}. \tag{21}$$

C. SNR Coverage Probability

The probability of $\gamma_{i,u}^{\mathrm{LoS}} = 0$ is denoted by $\mathbb{P}_{\mathrm{r}}(\gamma_{i,u}^{\mathrm{LoS}} = 0)$, which can be calculated as follows:

$$\mathbb{P}_{\mathrm{r}}(\gamma_{i,u}^{\mathrm{LoS}} = 0) = \int_{l_1}^{l_{\max}} f(l_{i,H}) \mathbb{P}_{\mathrm{B}}(l_{i,H}) dl_{i,H}, \tag{22}$$

where $f(l_{i,H})$ denotes the probability density function (PDF) of the random variable $l_{i,H}$, while $l_{\max}$ is the maximum distance between the human user and the AP. When channel blockage does not occur, the PDF of $\gamma_{i,u}^{\mathrm{LoS}}$ is derived by:

$$f(\gamma_{i,u}^{\mathrm{LoS}} | \gamma_{i,u}^{\mathrm{LoS}} = 0) = f(\dot{\gamma}_{i,u}^{\mathrm{LoS}}) \left[1 - \frac{1}{2\pi} \int_0^{2\pi} \mathbb{P}_{\mathrm{B}}(l_{i,H}) d\theta_{u,H}\right], \tag{23}$$

where $f(\dot{\gamma}_{i,u}^{\mathrm{LoS}})$ is the PDF of $\dot{\gamma}_{i,u}^{\mathrm{LoS}}$, and $\theta_{u,H}$ is the angle between the line from AP to UE and the line from UE to human body. In (23), $l_{i,H}$ can be approximated by $l_{i,u}$, which

$$l_{i,u} = \sqrt{\left[\frac{(m+1)A_{\text{pd}}(h_{i,H})^{m+1} g_f g_c R_{\text{pd}} P_{\text{mod}}}{2\pi\sqrt{\dot{\gamma}^{i,u}_{\text{LoS}} N_{\text{VLC}} B_{\text{VLC}}}}\right]^{\frac{2}{m+3}} - (h_{i,H})^2}. \tag{24}$$

TABLE I
SIMULATION PARAMETERS

Parameter	Value
The physical area of the PD, A_{pd}	1 cm^2
The gain of the optical filter, g_f	1
Refractive index, n	1.5
Half-intensity radiation angle, $\Phi_{1/2}$	60°
FoV semi-angle of the PD, Ψ_{max}	90°
Modulated optical power, P_{mod}	1 Watt
Detector responsivity, R_{pd}	0.53 A/W
Wall reflectivity, ρ_w	0.8
Bandwidth per VLC AP, B_{VLC}	20 MHz
PSD of noise in VLC, N_{VLC}	10^{-21} A^2/Hz

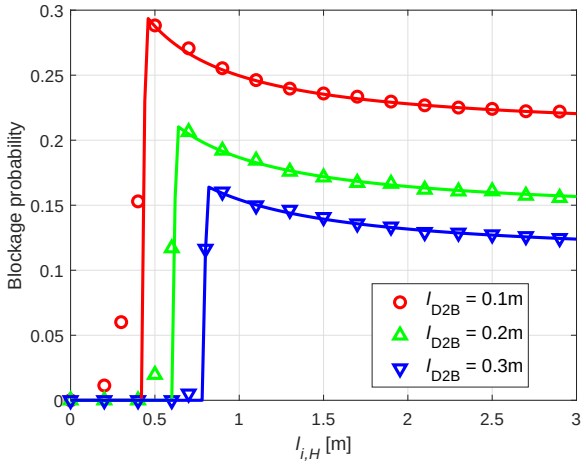

Fig. 3. Blockage probability of LoS (lines: analytical results, markers: simulations).

is computed as a function of $\dot{\gamma}^{\text{LoS}}_{i,u}$ in (24). Accordingly, (23) can be approximated to be:

$$\hat{f}(\gamma^{\text{LoS}}_{i,u}) = f(l_{i,u}(\dot{\gamma}^{\text{LoS}}_{i,u}))\left[1 - \mathbb{P}_{\text{B}}(l_{i,u}(\dot{\gamma}^{\text{LoS}}_{i,u}))\right]. \tag{25}$$

The normalised PDF of $\gamma^{\text{LoS}}_{i,u}$ for $\gamma^{\text{LoS}}_{i,u} \neq 0$ is obtained by:

$$f(\gamma^{\text{LoS}}_{i,u}|\gamma^{\text{LoS}}_{i,u} \neq 0) = \frac{1 - \mathbb{P}_{\text{r}}(\gamma^{\text{LoS}}_{i,u} = 0)}{\int_0^{l_{\text{max}}} \hat{f}(\gamma^{\text{LoS}}_{i,u}) dl_{i,u}} \hat{f}(\gamma^{\text{LoS}}_{i,u}). \tag{26}$$

IV. SIMULATION RESULTS

In this section, Monte Carlo simulations are carried out in MATLAB to evaluate the impact of human blockage on the UE's SNR coverage. The UE is randomly located in a room with uniform distribution. The room size is 5m by 5m, with a ceiling height of 2.6m. An average height of 1.7m is considered for the human body with a 0.3m body diameter, while the value of h_H is set to be 0.5m. Other parameters are summarised in Table I. For the LoS blockage, the simulation checks whether the direct path between UE and AP is blocked by human body. As for the NLoS blockage, it checks each reflection path and accumulates those paths that are not blocked.

A. Single VLC AP with LoS only

Fig. 3 shows the blockage probability as a function of $l_{i,H}$ for different values of the horizontal distance between device and body, which is denoted by $l_{\text{D2B}} = r_H - d_H/2$. As shown, the analytical expression in (21) largely agrees with the simulation results, expect it exhibits a sharper increase when $l_{i,H}$ is small. This is because when the human body is right below the AP, the shadow area is an ellipse instead of a trapezoid. When $l_{i,H}$ increases, the blockage probability first increases and then decreases. This is because when $l_{i,H}$ just becomes larger than l_1, the arc angle that would cause blockage (i.e., $\theta - \phi$) increases with $l_{i,H}$. When $l_{i,H}$ keeps increasing and becomes larger than l_2, this arc angle turns to be θ, which reduces as $l_{i,H}$ increases. Also, the blockage probability becomes higher for a smaller l_{D2B}, as expected. Taking $l_{i,H} = 3$m as an example, the chance of human blockage is about 22% when $l_{\text{D2B}} = 10$cm, while for $l_{\text{D2B}} = 30$cm the chance reduces to only 12%.

The coverage probability of LoS SNR with a single AP is presented in Fig. 4 when l_{max} is set to be 2.5m. As shown, in general, the analytical expression in (26) closely matches the simulation results. At the lower end of SNR, the derived expression slightly deviates from the simulations, especially for a large l_{D2B}. This is a result of using $l_{i,u}$ to approximate $l_{i,H}$, and this approximation is more accurate for a smaller l_{D2B}. When l_{D2B} increase, the coverage probability of LoS SNR increases towards the case of no blockage. For instance, when $l_{\text{D2B}} = 10$cm, the 50th percentile of LoS SNR is 2.3 dB less than that of no blockage. This gap reduces to only 0.7 dB when l_{D2B} increases to 30cm.

B. VLC Network with LoS and NLoS

Fig. 5 presents the coverage probability of LoS SNR when there are 4 APs in the room, with l_{D2B} fixed to be 10cm. Let d_{AP} denote the distance between two nearest APs. Unlike in Fig. 4, the lower end of CDF in Fig. 5 starts from zero probability. This indicates that when the human body blocks the UE from the nearest AP, the UE can still have access to another AP. However, this degrades SNR compared with the case of no blockage. As shown, this degradation becomes more significant when d_{AP} increases. Taking $d_{\text{AP}} = 2$m as an example, the 50th percentile of LoS SNR is 0.4 dB less

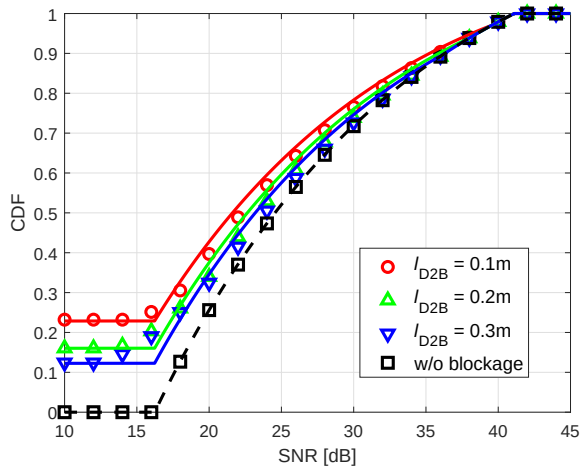

Fig. 4. Coverage probability of LoS SNR with a single AP (lines: analytical results, markers: simulations).

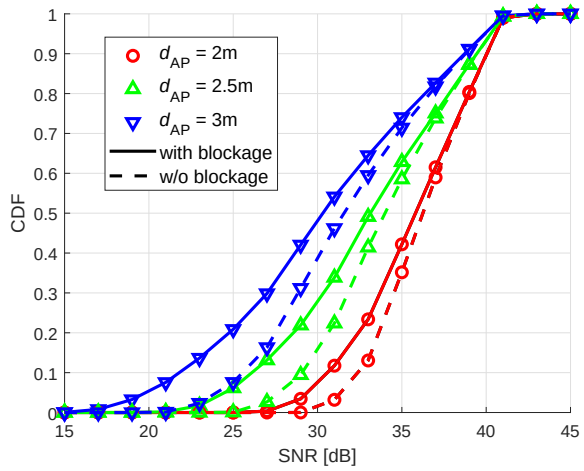

Fig. 5. Coverage probability of LoS SNR with 4 APs (simulations).

than that of no blockage. This gap increases to 1.3 dB for $d_{\mathrm{AP}} = 3$m. The coverage probability of NLoS SNR is studied in Fig. 6. Human blockage causes a decrease of 2.5dB to NLoS SNR, regardless of d_{AP}. However, the value of NLoS SNR becomes higher when d_{AP} increases, since in this case the APs are closer to the wall, leading to stronger reflections.

V. Conclusion

In this paper, a closed-form expression was derived for the coverage probability of LoS SNR under the impact of human blockage, with a particular analysis of the distance between human body and UE. The derived expressions closely match the simulation results, which also show that increasing the distance between body and device from 10cm to 30cm can nearly halve the blockage probability and increase the 50-th percentile LoS SNR by 1.6 dB. Decreasing the separation between APs can reduce the LoS SNR degradation caused by human blockage but barely affects the degradation of NLoS

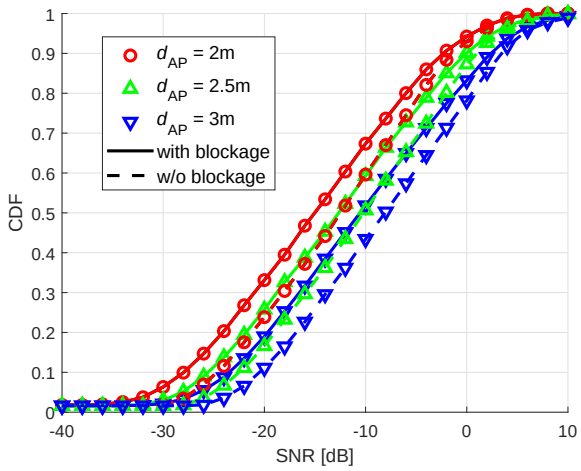

Fig. 6. Coverage probability of NLoS SNR with 4 APs (simulations).

SNR. Future work will investigate how the SNR performance of one UE is affected by the human bodies of other UEs.

Acknowledgement

This work was supported by the Seed Funding Scheme of University College Dublin.

References

[1] H. Burchardt, N. Serafimovski, D. Tsonev, S. Videv, and H. Haas, "VLC: Beyond point-to-point communication," *IEEE Commun. Mag.*, vol. 52, no. 7, pp. 98–105, Jul. 2014.

[2] H. Zhang, A. Yang, L. Feng, and P. Guo, "Gb/s real-time visible light communication system based on white LEDs using T-bridge cascaded pre-equalization circuit," *IEEE Photon. J.*, vol. 10, no. 2, pp. 1–7, 2018.

[3] X. Wu, M. D. Soltani, L. Zhou, M. Safari, and H. Haas, "Hybrid LiFi and WiFi networks: A survey," *IEEE Commun. Surveys Tuts.*, vol. 23, no. 2, pp. 1398–1420, 2021.

[4] X. Wu and H. Haas, "Handover skipping for LiFi," *IEEE Access*, vol. 7, pp. 38 369–38 378, 2019.

[5] K. Ji, T. Mao, J. Chen, Y. Dong, and Z. Wang, "SVM-based network access type decision in hybrid LiFi and WiFi networks," in *2019 IEEE 90th Vehicular Technology Conf. (VTC2019-Fall)*, Honolulu, HI, 2019.

[6] X. Wu and H. Haas, "Load balancing for hybrid LiFi and WiFi networks: To tackle user mobility and light-path blockage," *IEEE Trans. Commun.*, vol. 68, no. 3, pp. 1675–1683, Mar. 2020.

[7] V. Rodoplu, K. Hocaoğlu, A. Adar, R. O. Çikmazel, and A. Saylam, "Characterization of line-of-sight link availability in indoor visible light communication networks based on the behavior of human users," *IEEE Access*, vol. 8, pp. 39 336–39 348, 2020.

[8] S. Jivkova and M. Kavehrad, "Shadowing and blockage in indoor optical wireless communications," in *2003 IEEE Global Telecommunications Conf. (GLOBECOM)*, vol. 6, San Francisco, CA, 2003, pp. 3269–3273.

[9] A. Singh, G. Ghatak, A. Srivastava, V. A. Bohara, and A. K. Jagadeesan, "Performance analysis of indoor communication system using off-the-shelf leds with human blockages," *IEEE Open Journal of the Communications Society*, vol. 2, pp. 187–198, 2021.

[10] C. Chen, D. A. Basnayaka, A. A. Purwita, X. Wu, and H. Haas, "Wireless infrared-based LiFi uplink transmission with link blockage and random device orientation," *IEEE Trans. Commun.*, vol. 69, no. 2, pp. 1175–1188, 2021.

[11] C. Chen, D. A. Basnayaka, X. Wu, and H. Haas, "Efficient analytical calculation of non-line-of-sight channel impulse response in visible light communications," *J. Lightw. Technol.*, vol. 36, no. 9, pp. 1666–1682, 2018.

[12] J. Kahn and J. Barry, "Wireless infrared communications," *Proc. IEEE*, vol. 85, no. 2, pp. 265–298, Feb. 1997.